Quantification of Aquaporin-CHIP water channel protein in microdissected renal tubules by fluorescence-based ELISA.

Y Maeda, … , P Agre, M A Knepper

Research Article

Several transporters have been localized along the nephron by physiological methods or immunocytochemistry. However, the actual abundance of these molecules has not been established. To accomplish this goal, we have developed a fluorescence-based ELISA method and have used it to quantitate Aquaporin-CHIP (AQP-CHIP) water channel protein in rat kidney tubules. Microdissected tubules (2 mm/sample, permeabilized with 0.5% Triton X-100) or purified AQP-CHIP standards (0-200 fmol) were utilized in a fluorescence ELISA protocol after covalent immobilization on epoxy-activated Sepharose beads. The lower limit of detection was 2.4 fmol of AQP-CHIP. Preabsorption with excess purified AQP-CHIP or use of nonimmune serum eliminated the signal. In proximal segments, the measured AQP-CHIP was linearly related to tubule length (1-10 mm). The measured AQP-CHIP was (mean +/- SE, fmol/mm): S-1 proximal, 10.8 +/- 2.1; S-2, 10.0 +/- 2.3; S-3, 21.3 +/- 3.1; type 1 thin descending limb (DTL), 12.9 +/- 4.6; type 2 DTL, 86.5 +/- 19.5; type 3 DTL, 43.0 +/- 11.2. In thin ascending limbs, thick ascending limbs, distal convoluted tubules, connecting tubules, and collecting ducts, the AQP-CHIP signal was indistinguishable from zero. Based on the unit water conductance of single CHIP molecules, our calculations show that the content of AQP-CHIP is sufficient to explain water permeability measured in isolated proximal tubules and DTL segments.

Find the latest version:

Quantification of Aquaporin-CHIP Water Channel Protein in Microdissected Renal Tubules by Fluorescence-based ELISA

Yoshitaka Maeda, Barbara L. Smith,* Peter Agre,* and Mark A. Knepper

Laboratory of Kidney and Electrolyte Metabolism, National Heart, Lung and Blood Institute, National Institutes of Health, Bethesda, Maryland 20892-1598; and *Department of Biological Chemistry, Johns Hopkins University School of Medicine, Baltimore, Maryland 21205

Abstract

Several transporters have been localized along the nephron by physiological methods or immunocytochemistry. However, the actual abundance of these molecules has not been established. To accomplish this goal, we have developed a fluorescence-based ELISA method and have used it to quantitate Aquaporin-CHIP (AQP-CHIP) water channel protein in rat kidney tubules. Microdissected tubules (2 mm/sample, permeabilized with 0.5% Triton X-100) or purified AQP-CHIP standards (0–200 fmol) were utilized in a fluorescence ELISA protocol after covalent immobilization on epoxy-activated Sepharose beads. The lower limit of detection was 2.4 fmol of AQP-CHIP. Preabsorption with excess purified AQP-CHIP or use of nonimmune serum eliminated the signal. In proximal segments, the measured AQP-CHIP was linearly related to tubule length (1–10 mm). The measured AQP-CHIP was (mean$\pm$SE, fmol/mm): S-1 proximal, 10.8$\pm$2.1; S-2, 10.0$\pm$2.3; S-3, 21.3$\pm$3.1; type 1 thin descending limb (DTL), 12.9$\pm$4.6; type 2 DTL, 86.5$\pm$19.5; type 3 DTL, 43.0$\pm$11.2. In thin ascending limbs, thick ascending limbs, distal convoluted tubules, connecting tubules, and collecting ducts, the AQP-CHIP signal was indistinguishable from zero. Based on the unit water conductance of single CHIP molecules, our calculations show that the content of AQP-CHIP is sufficient to explain water permeability measured in isolated proximal tubules and DTL segments. (*J. Clin. Invest.* 1995. 95:422–428.) Key words: proximal tubule • loop of Henle • collecting duct • nephron • water channel

Introduction

The renal tubule is composed of a series of distinct segments, each with specialized transport function. The multiplicity of renal tubule segments allows the kidney to simultaneously regulate the excretion of numerous substances (1). The character of each individual renal tubule segment with regard to transport capacity for various substances is determined by the extent of expression of corresponding transporter proteins, e.g., Na, K-ATPase, glucose transporters, ion channels, and water channels. Although the relative expression of various transporters has been evaluated by physiological methods or by immunohistochemistry, quantitative methods for measurement of the abundance of the transporters in individual tubule segments have not been available. In this paper, we describe an approach capable of measuring the amounts of specific proteins in microdissected renal tubules and apply it to measurement of the abundance of the water channel Aquaporin-CHIP (AQP-CHIP)[1] along the nephron.

AQP-CHIP is a molecular water channel expressed in kidney, erythrocytes, choroid plexus of the brain, and several other tissues (2). Immunohistochemical studies of kidney have demonstrated that it is found in both the renal proximal tubule and descending limb of Henle's loop (3–5) where it is proposed to play an important role in fluid absorption. After the identification of AQP-CHIP and the cloning of its cDNA, several analogous aquaporins that are expressed in the kidney have been identified (6). Measurement of the abundance of these water channel proteins in nephron and collecting duct segments is an important goal which, when met, will allow an assessment of the functional roles of these proteins in the mediation of water transport in each segment. The fluorescence-based ELISA method for quantification of AQP-CHIP in microdissected tubules described in this paper has a detection threshold of 2.4 fmol, a sensitivity sufficient to allow for quantification of AQP-CHIP in 1–2 mm of microdissected tubules. We apply the method to address whether the levels of AQP-CHIP expression in the proximal tubule and thin descending limb are sufficient to account for water permeabilities measured in isolated perfused tubules.

Methods

Antibodies and purified AQP-CHIP. AQP-CHIP protein was purified as described previously (7). The concentration of AQP-CHIP in the stock solution used for standards was measured by the BCA method (Pierce, Rockford, IL). Residual reducing activity due to dithiothreitol was removed by bubbling the solution with 100% O_2.

Address correspondence to Mark A. Knepper, M.D., Ph.D., Laboratory of Kidney and Electrolyte Metabolism, Building 10, Room 6N307, National Institutes of Health, Bethesda, MD 20892-1598. Phone: 301-496-3064; FAX: 301-402-1443.

1. *Abbreviations used in this paper:* AQP-CHIP, aquaporin-CHIP; CD, collecting duct; DTL, descending thin limb; MUG, 4-methylumbelliferyl-β-D-galactopyranoside.

All antisera were used at a 1:500 dilution unless indicated otherwise. Rabbit anti–human AQP-CHIP serum (anti–AQP-CHIP) was characterized previously (5). Polypeptide preabsorption was carried out by incubating 500 μl of 1:500 anti–AQP-CHIP with 6.35 μg of purified AQP-CHIP overnight at 4°C. Nonimmune serum was supplied by Lofstrand Laboratories, Inc. (Gaithersburg, MD).

Solutions. Bicarbonate-buffered physiological saline contained (mM): NaCl, 117; KCl, 4; NaH$_2$PO$_4$, 2; CaCl$_2$, 2; MgSO$_4$, 1.2; CH$_3$COONa, 5; NaHCO$_3$, 25; glucose, 5.5 (plus 0.1% bovine serum albumin). Hepes-buffered physiological saline contained (mM):NaCl, 142; KCl, 4; NaH$_2$PO$_4$, 2; MgSO$_4$, 1.2; CaCl$_2$, 2; Na acetate, 5; Hepes, 5; glucose, 5.5 (pH 7.4). The Triton/Hepes buffer solution contained (mM): NaCl, 74; KCl, 2, NaH$_2$PO$_4$, 1; MgSO$_4$, 0.6; CaCl$_2$, 1; CH$_3$COONa, 2.5; Hepes, 2.5; glucose, 2.75; plus Triton X-100 (0–4%) and 0.01% NaN$_3$ (pH 7.4). Sodium phosphate buffer contained 0.1 M sodium phosphate, 0.5 M NaCl, and 0.1% Tween 20 (pH 7.4).

Experimental animals and tissue preparation. Pathogen-free Sprague-Dawley rats (200–250 g body weight; Taconic Farms Inc., Germantown, NY) were maintained on an ad libitum intake of standard rat chow (NIH-31 autoclavable rodent diet; Zeigler Brothers, Inc., Gardners, PA) and water. The kidneys were prepared for microdissection as reported previously (8) and as briefly reiterated in the following. The rats were injected with furosemide (5 mg intraperitoneally) 30 min before decapitation. To perfuse the left kidney in isolation, the abdominal aorta was cannulated with polyethylene tubing (PE90) below the left kidney and was ligated above the left renal artery. The kidney was perfused initially with 10 ml ice-cold bicarbonate-buffered physiological saline. This solution was equilibrated with 95% O$_2$/5% CO$_2$. Next, the kidney was perfused over 10 min with 23 ml of bicarbonate-buffered physiological saline containing 2 mg/ml of collagenase (collagenase B; Boehringer-Mannheim Biochemicals, Indianapolis, IN). The perfused kidney was resected and a coronal slice of kidney containing the cortico-papillary axis was transferred to bicarbonate-buffered physiological saline containing 2 mg/ml collagenase for 15 min at 37°C with agitation on a rotary shaker. The tissue was washed with chilled Hepes-bufferend physiological saline and transferred for microdissection.

Tubule microdissection. Nephron and collecting duct segments were dissected from collagenase-treated tissue as described previously (8, 9). Briefly, the tubules were teased from either cortex, outer medulla, or inner medulla using Dumont No. 5 forceps under a Wild M-8 dissecting microscope in transmitted-light mode. The dissection medium was Hepes-buffered physiological saline at 12°C. The terminology and abbreviations used for proximal tubule and loop of Henle segments are summarized in Fig. 1. The tubule segments were identified by their appearance and location based on previously described criteria (9). Collecting ducts (CD) are referred to by their region of origin (cortex, CCD; outer medulla, OMCD; inner medulla, IMCD). The lengths of individual microdissected segments were determined using a calibrated eyepiece micrometer. The tubules were transferred from the dissection dish to ELISA microplates in 5 μl of dissection fluid using a small glass capillary.

ELISA. AQP-CHIP was quantified by an ELISA with fluorescence endpoint as described in the following. The assay uses filter-bottom 96-well microtiter plates (MultiScreen-HV; Millipore Corp., Bedford, MA). In these plates, the filter bottom is constructed of hydrophilic Durapore membranes (0.45 μm pore size) selected for low protein binding. Filter-bottom plates allow rapid washing and solution exchange through use of a vacuum manifold (MultiScreen vacuum manifold; Millipore Corp.). 10 mg of epoxy-activated Sepharose (6B; Pharmacia LKB Biotechnology, Piscataway, NJ) was mixed with 1 ml of water and agitated for 15 min at room temperature. 10 μl of this suspension was transferred per well of the 96-well plate, followed by five washes with 200 μl of water. Just before introduction of standards or samples, the fluid was removed by filtration. For standards, known quantities of purified AQP-CHIP dissolved in 10 μl of 0.5% Triton X-100/Hepes buffer (with 0.01% NaN$_3$) were transferred to individual wells preloaded with epoxy-activated Sepharose. For tubule samples, microdissected tubule segments were transferred in 5 μl Hepes dissection buffer into wells preloaded with 5 μl of 1% Triton X-100/Hepes containing 0.02% NaN$_3$, giving a final Triton X-100 concentration of 0.5%. The optimal Triton X-100 concentration was determined experimentally (see Results). After the standards or samples were incubated for 1 h at room temperature, 40 μl of 2 M potassium phosphate (pH 8; containing 0.01% NaN$_3$) was added. The microtiter plate was then incubated overnight at room temperature with agitation on a rotary shaker to allow the immobilization reaction to occur.

After overnight incubation, each well was washed once with 2 M potassium phosphate and then incubated with 1 M ethanolamine dissolved in 0.1 M potassium phosphate (pH 8) for 6 h at room temperature to inactivate the residual active sites of the epoxy-activated Sepharose. Unbound ethanolamine was washed away by sequential washes with 0.1 M acetate buffer (pH 4, in 0.5 M NaCl) and 0.1 M Tris/HCl buffer (pH 8, in 0.5 M NaCl), repeated twice. Next, 50 μl of a 1:500 dilution of anti–AQP-CHIP in sodium phosphate buffer was added to each well, and the microplate was incubated overnight at 4°C with agitation on a rotary shaker.

After overnight incubation, each well was washed three times with sodium phosphate buffer. Next, donkey anti–rabbit immunoglobulin conjugated to β-galactosidase (Amersham Corp., Arlington Heights, IL) was added to each well at a 1:2,000 dilution in sodium phosphate buffer, and the samples were incubated for 1 h at room temperature. Then, the samples were washed again three times with 200 μl of sodium phosphate buffer, followed by two additional washes with the same buffer without Tween 20. Next, a fluorogenic substrate for β-galactosidase, 4-methylumbelliferyl-β-D-galactopyranoside (MUG), was added to each well (50 μl of 0.1 M MUG in isotonic phosphate-buffered saline containing 1 mM MgSO$_4$ and 0.1% BSA pH 7.2). After a 30-min incubation at room temperature, the enzyme reaction was stopped by the addition of 150 μl of 0.1 M glycine (pH 10.3). The samples were diluted with 250 μl of water, and the fluorescence was read in a 400-μl quartz cuvet on a SPEX FluoroMax spectrofluorometer (SPEX Industries, Inc., Edison, NJ) (excitation: 360 nm; emission, 440 nm; slit width, 1 nm). Fluorescence intensity was read as photon counts per second (cps). The blank values, which were generated by carrying out the 30-min MUG incubation in the absence of β-galactosidase, were subtracted from the measured fluorescence intensity of the samples. The blank value for nine successive assays reported in this paper averaged 0.97±0.02 × 10^6 cps. The amount of AQP-CHIP was calculated from the fluorescence intensity of samples using a standard curve of purified AQP-CHIP generated in each assay.

Results

Effect of Triton X-100 concentration on AQP-CHIP detection. The anti–AQP-CHIP recognizes predominantly the COOH-terminal tail of AQP-CHIP which is located in the cytoplasm (5). Thus, the assay requires a means of exposing the intracellular domains of AQP-CHIP to the antibody. The cells are undoubtedly permeabilized by osmotic shock as demonstrated previously (10) as the tubules are transferred into the hypotonic Triton/Hepes solution followed by exchange to 2 M potassium phosphate. In addition, we use detergents to assure permeabilization and partial solubilization of AQP-CHIP in microdissected tubules. Preliminary studies indicated that Triton X-100 was more effective than either SDS or Tween 20 for this purpose. Fig. 2 shows the effect of Triton X-100 concentration on the fluorescence signal obtained by application of the ELISA to microdissected S-3 proximal tubules. The signal was maximized at low values of Triton X-100 concentration (0–0.5%). Subsequent studies used 0.5% Triton X-100.

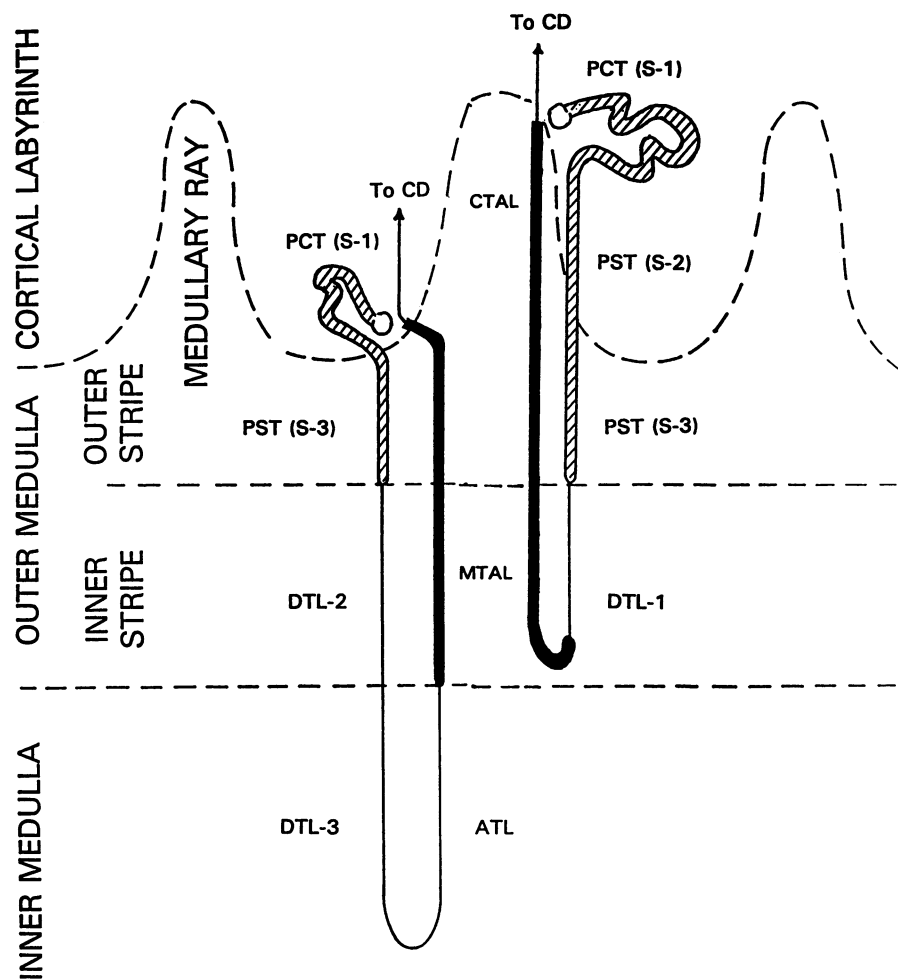*Specificity.* Fig. 3 shows the signals obtained with purified

Figure 1. Terminology for nephron segments. Diagram depicts a long-looped nephron (*left*) and a short-looped nephron (*right*). PCT *(S-1)*, early proximal convoluted tubule; PST *(S-2)*, early proximal straight tubule; PST *(S-3)*, late proximal straight tubule; DTL-1, descending thin limb of short loop; DTL-2, descending thin limb of long loop (outer medullary); DTL-3, descending thin limb of long loop (inner medullary); ATL, ascending thin limb; TAL, thick ascending limb. See text for dissection and identification criteria.

AQP-CHIP standards and microdissected S-3 proximal tubules using anti–AQP-CHIP, anti–AQP-CHIP preabsorbed with purified AQP-CHIP, and with nonimmune rabbit serum as the primary antibody in the ELISA protocol. As shown, the signal was decreased 90% or more with preabsorbed or nonimmune serum, indicating a high degree of specificity of the assay.

Standard curve. A standard curve was generated for each assay. Fig. 4 shows a typical standard curve using purified AQP-CHIP. The detection limit (defined as three standard deviations above the background signal) was seen at ~ 2.4 fmol (or 68 pg). The background signal averaged $5.18 \pm 0.39 \times 10^6$ cps for all experiments. The coefficient of variation ranged from 9 to 18% for all standards. In general, standards were not run above 200 fmol because fluorescence self-quenching occurred at very high fluorescence levels (i.e., $> 70 \times 10^6$ cps).

Dependence on tubule length. If the ELISA method yields an unbiased measure of the quantity of AQP-CHIP protein, the total amount of AQP-CHIP detected should be linearly related to tubule length. Fig. 5 shows the measured AQP-CHIP in different lengths of S-3 proximal tubule ranging from 1 to 10 mm. As shown, the relationship between AQP-CHIP detected and tubule length was approximately linear, supporting the validity of the assay.

Quantification of AQP-CHIP along the renal tubule. The quantity of AQP-CHIP protein was measured in 14 different renal tubule segments dissected from the kidneys of 5 normal rats. Fig. 6 shows the results obtained in proximal tubule and loop of Henle segments expressed as femtomoles of AQP-CHIP per millimeter length of tubule. Values were above the nominal detection limit (2.4 fmol) only in the three proximal segments (S-1, S-2, and S-3) and in the three thin descending limb segments (DTL-1, DTL-2, and DTL-3). Values were highest in the two thin descending limb segments associated with long-loop nephrons (DTL-2 and DTL-3). Expressed as number of molecules per tubule length, the values were (molecules/mm $\times 10^9$): S-1, 6.5 ± 1.3; S-2, 6.0 ± 1.4; S-3, 12.8 ± 1.9; DTL-1, 7.8 ± 2.8; DTL-2, 52.1 ± 11.7; DTL-3, 25.9 ± 6.8. In the ascending limb segments (ascending thin limb, medullary thick ascending limb, and cortical thick ascending limb), AQP-CHIP was undetectable. Furthermore, in distal convoluted tubule ($n = 4$), connecting tubules ($n = 3$), cortical collecting ducts ($n = 5$), outer medullary collecting ducts ($n = 6$), and inner medullary collecting ducts ($n = 6$), the AQP-CHIP was below the detection limit.

Discussion

ELISA method. The investigation of renal function has benefitted in the past from scale-down of standard approaches to a sensitivity level applicable to short segments of microdissected
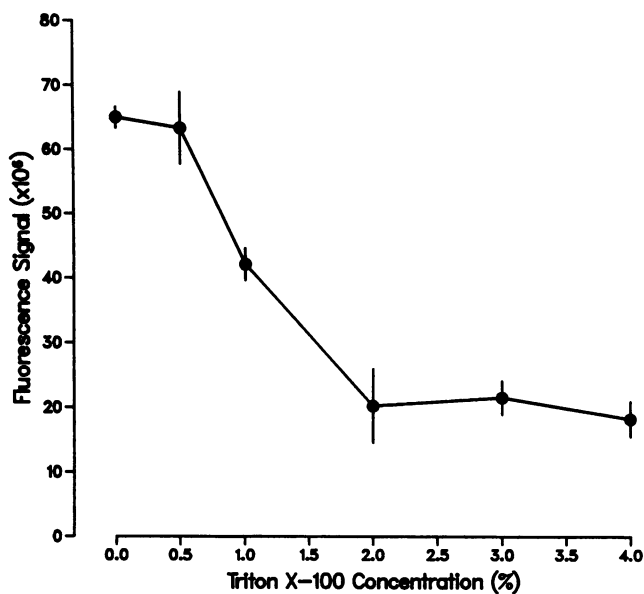
Figure 2. Effect of Triton X-100 concentration on fluorescence signal obtained from microdissected S-3 segments (5 mm each). Background fluorescence values in absence of tubules were subtracted. Anti–AQP-CHIP was used at 1:250 dilution in these experiments. Values are mean±SE.

Figure 3. Specificity of AQP-CHIP determinations. Experiments used purified AQP-CHIP standards (50 fmol/sample, *left*) and S-3 proximal tubules (5 mm/sample, *right*). Anti–AQP-CHIP and nonimmune serum were used at a dilution of 1:500. Preabsorption was accomplished by incubation of 50 μl of 1:500 anti–AQP-CHIP with 6.35 μg of purified AQP-CHIP overnight at 4°C. Values are mean±SE.

tubule. Such techniques have allowed a detailed mapping of the functional and biochemical properties of the renal tubule. In this paper, we introduce a new single-tubule method which is capable of measuring the quantities of specific proteins in microdissected tubule segments based on immunodetection. This approach is configured as an ELISA with a fluorometric readout. We demonstrate in this paper that, when applied to the detection of the water channel AQP-CHIP, this assay method has a detection threshold of ~ 2.4 fmol, a sensitivity sufficient to efficiently quantify AQP-CHIP in 1–2 mm of microdissected proximal tubules or descending limbs of Henle. In contrast, Western blotting, which is only semiquantitative, is capable of detecting ~ 1–10 ng of AQP-CHIP (5). Thus, the fluorescence-based ELISA method used here is at least two to three orders of magnitude more sensitive than Western blotting for detection of AQP-CHIP. Although we have only attempted to apply this method to measurement of AQP-CHIP, it should be applicable to the detection of other proteins at a single tubule level as well, providing that they are present in at femtomole per milliliter levels in the renal tubule and providing that a specific, high-affinity antibody is available.

Extensive preliminary studies were carried out to optimize the sensitivity and detection limit of the assay. The factors considered included: the type and concentration of detergent used for permeabilization of tubules, the choice of immobilization medium, the immobilization conditions, the conditions for exposure to the primary antibody including the dilution factor, the concentration of secondary antibody, and the conditions for incubation with the fluorescent substrate (MUG). Among these, the conditions for permeabilization and immobilization appear to be the most critical. The permeabilization is accomplished in part by osmotic shock, abetted by the addition of a nonionic detergent, Triton X-100, to the permeabilization medium. The
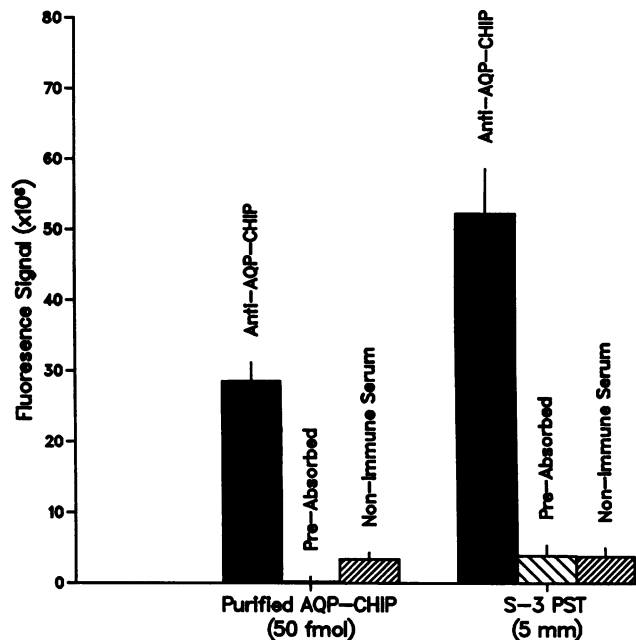
use of detergents, however, necessitated a covalent immobilization procedure since detergents can markedly impair noncovalent interactions with hydrophobic membranes. The immobilization was enhanced by use of a hypertonic immobilization medium (2 M potassium phosphate) as described previously (11). High concentrations of Triton X-100 markedly diminished the fluorescent signal from microdissected tubules (Fig. 2), possibly by interfering with the immobilization process.

AQP-CHIP quantitation in single renal tubule segments. The qualitative pattern of AQP-CHIP expression along the renal tubule is in complete agreement with prior immunohistochemical studies (3–5). Measurable expression was seen only in the proximal tubule and thin descending limb of Henle's loop, consistent with the view that AQP-CHIP is the major water channel of the nephron segments whose cells have constitutively high osmotic water permeability values. The absence of measurable AQP-CHIP in the ascending limb of the loop of Henle, in the distal convoluted tubule, and in the connecting tubule is consistent with the low epithelial osmotic water permeability values measured in these segments (12). Furthermore, the absence of measurable AQP-CHIP in collecting duct segments is consistent with immunocytochemical findings (5) in a segment whose vasopressin-dependent water permeability is believed to be attributable to a different water channel, AQP-CHIP (13, 14). Thus, from a qualitative point of view, our results are wholly confirmatory of prior immunolocalization studies. Quantitatively, the highest level of expression of AQP-CHIP (normalized by tubule length) was found in the descending thin limbs of the long loop of Henle, both the outer medullary (DTL-2) and inner medullary (DTL-3) segments. Osmotically driven water absorption from these segments is thought to play a cru-
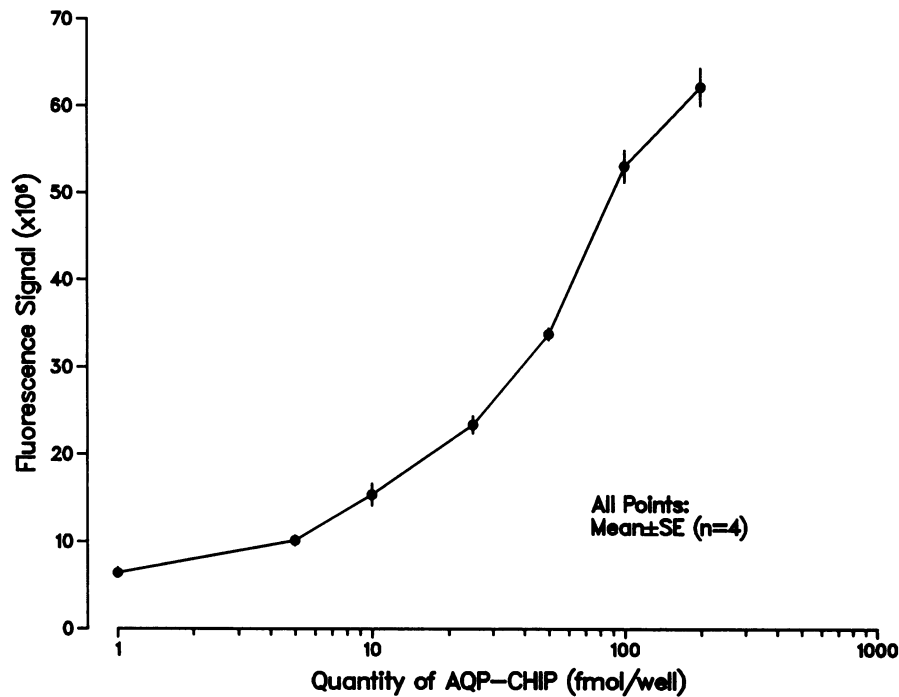
Figure 4. Typical standard curve for fluorescence-based ELISA. Standards are purified AQP-CHIP (see text). Values are mean±SE ($n = 4$ for each point).

cial role in the urinary concentrating mechanism, and even a small lag in osmotic equilibration across the long-loop descending limb may significantly dissipate the cortico-medullary osmotic gradient (12). Thus, the very high level of AQP-CHIP expression seen in the long-loop descending limb may be critical to the ability of the kidney to excrete a maximally concentrated urine. The level of expression of AQP-CHIP in the de-
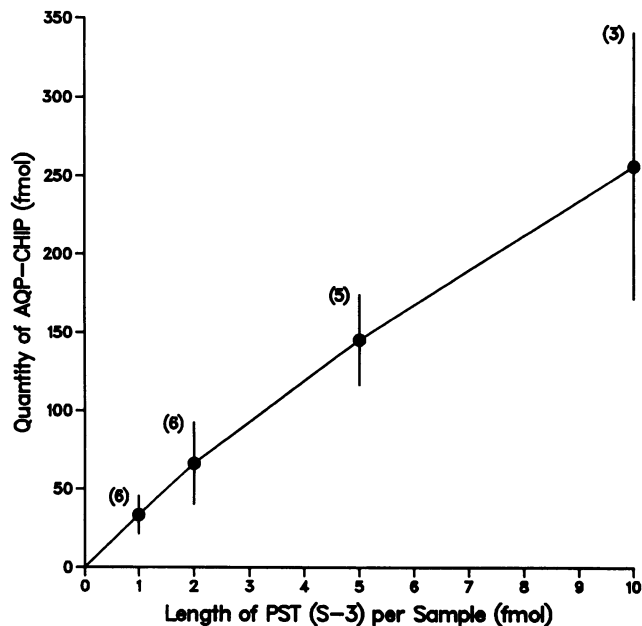

Figure 5. Relationship between measured AQP-CHIP content and total tubule length per sample. Each value represents mean±SE. Number of determinations is indicated in parentheses.

scending limb of short loops of Henle (DTL-1) was low relative to that seen in the long-loop descending limbs. This observation is consistent with recent immunohistochemical findings showing a marked decrease in AQP-CHIP labeling in the late portion of DTL-1 (15). Unfortunately, this segment is difficult to perfuse in vitro and insufficient information is available to judge whether the water permeability is significantly lower in DTL-1 than in DTL-2 (16). Aside from the thin descending limb, the other major site of AQP-CHIP expression in the kidney is the proximal tubule. Substantial levels of AQP-CHIP were detected in all three proximal tubule subsegments (S-1, S-2, and S-3). The proximal tubule is the major site of water absorption along the nephron, accounting for approximately two-thirds of renal water absorption. Fluid absorption occurs virtually isosmotically in the proximal tubule/ because the high epithelial water permeability allows rapid water fluxes in response to miniscule osmotic gradients. Consequently, when NaCl is actively absorbed, water follows efficiently. Thus, the high level of AQP-CHIP expression in the proximal tubule is critical to the efficient absorption of the glomerular filtrate. The higher level of AQP-CHIP in S-3 than in S-1 and S-2 proximal tubules correlates well with the apparently higher density of labeling in S-3 seen by immunohistochemistry (5).

Although our ELISA detects a substantial quantity of AQP-CHIP in the proximal tubule, the amount appears low in comparison with levels seen in the long-loop descending limb. This raises the question of whether the proximal tubule contains a sufficient level of AQP-CHIP to account for the observed osmotic water permeability. Using methods optimized for the accurate determination of osmotic water permeability in the proximal tubule, both Preisig and Berry (17) and Green and Giebisch (18) found values in the range of 1,000–1,500 μm/s. To calculate the osmotic water permeability predicted from the measured level of AQP-CHIP in the S-1 proximal tubule, we can use the
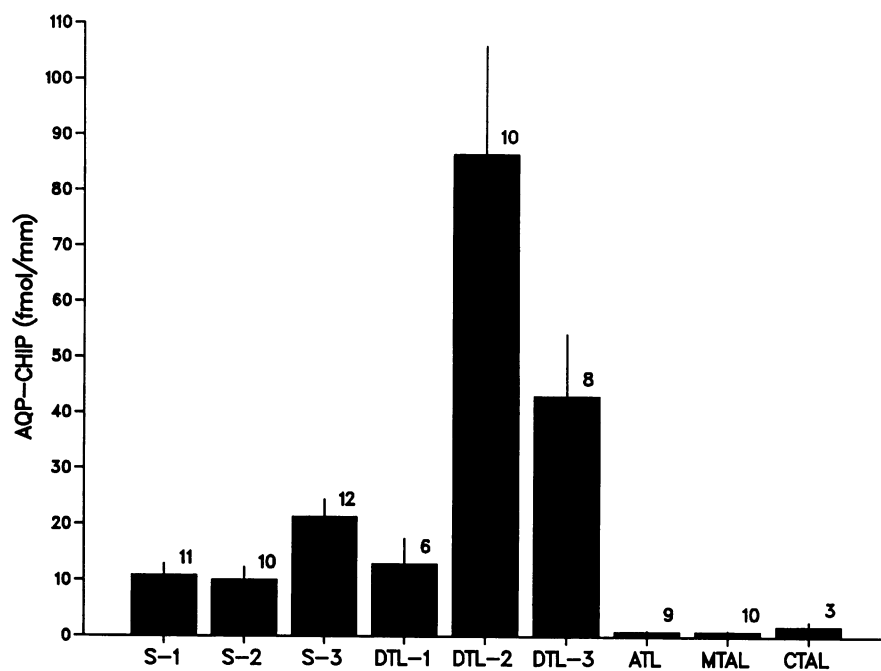
Figure 6. AQP-CHIP content in individual microdissected renal tubule segments. Each sample used 2 mm of the indicated segment. Number of determinations is indicated above each bar. Abbreviations as in Fig. 1.

unit water conductance (p_f) of a single AQP-CHIP monomer reported in the reconstitution studies of Zeidel et al. (19) and Van Hoek and Verkman (20), i.e., 10^{-13} cm^3/(s·molecule). The maximum estimate would be obtained if the measured AQP-CHIP were equally divided between the apical and basolateral plasma membranes of the proximal tubule cells. Under this assumption, the amount of AQP-CHIP present in the apical membrane of the S-1 proximal tubule would be half of the value shown in Fig. 6, viz. 5.4 fmol/mm, or (multiplying by Avogadro's number) 3.25×10^9 molecules/mm (N_a).[2] Assuming that the inner diameter of a proximal tubule is 25 μm, the nominal luminal surface area per unit length (S_A) would be 7.85×10^4 μm^2/mm. Thus, the water permeability of the apical barrier would be $P_{fa} = P_f \cdot N_a/S_A = 4,140$ μm/s. The epithelial permeability P_f can be calculated from the apical permeability (P_{fa}) and the basolateral permeability (P_{fb}) by assuming two resistances in series: $1/P_f = 1/P_{fa} + 1/P_{fb}$. If P_{fb} is assumed to be equal to P_{fa}, consistent with the assumption of equal amounts of AQP-CHIP in both membranes, then the overall epithelial water permeability (P_f) will be $1/P_{fa}$ or 2,070 μm/s. Thus, 2,070 μm/s is the maximum epithelial osmotic water permeability that can be explained by the measured amount of AQP-CHIP in the S-1 proximal tubule. Since this value is larger than the measured values in the proximal convoluted tubule, 1,000–1,500 μm/s (17, 18), it follows that the measured AQP-CHIP is adequate to account for the measured permeability. However, the calculation does not rule out the existence of another water channel that could contribute to the overall water permeability of the proximal tubule. Such a possibility is supported by the recent identification of three human subjects who do not express functional AQP-CHIP due to mutations in the *aquaporin-1* gene and yet do not exhibit major abnormalities in renal function (22). Furthermore, similar calculations (which will not be repeated here) establish that the measured amount of AQP-CHIP in the DTL-2 and DTL-3 segments is sufficient to account for measured permeabilities in the range of 1,500–3,000 μm/s (14, 23).

Acknowledgments

---

2. The number of AQP-CHIP molecules per cell can be estimated from N_a by multiplying by 2 (to get the total number of AQP-CHIP molecules per millimeter) and then dividing by the number of cells per unit length in the proximal convoluted tubule, $\sim$ 280 cells/mm (10). Thus, we can estimate that there are $\sim$ 20 million AQP-CHIP molecules per proximal tubule cell. For comparison, in erythrocytes there are $\sim$ 200,000 molecules per cell (7). The 100-fold greater AQP-CHIP expression per cell in proximal tubule cells versus erythrocytes may be due in part to the fact that the total membrane surface area of proximal tubules cells is much larger. Due to the presence of apical microvilli and complex cellular interdigitations, both the apical and basolateral plasma membrane surface areas are greatly amplified (21).

References

1. Knepper, M. A., and M. B. Burg. 1983. Organization of nephron function. *Am. J. Physiol.* 244:F579–F589.

2. Agre, P., G. M. Preston, B. L. Smith, J. S. Jung, S. Raina, C. Moon, W. B. Guggino, and S. Nielsen. 1993. Aquaporin CHIP: the archetypal molecular water channel. *Am. J. Physiol.* 265:F463–F476.

3. Denker, B. M., B. L. Smith, F. P. Kuhajda, and P. Agre. 1988. Identification, purification, and partial characterization of a novel M_r 28,000 integral membrane protein from erythrocytes and renal tubules. *J. Biol. Chem.* 263:15634–15642.

4. Sabolic, I., G. Valenti, J.-M. Verbavatz, A. N. Van Hoek, A. S. Verkman, D. A. Ausiello, and D. Brown. 1992. Localization of the CHIP28 water channel in rat kidney. *Am. J. Physiol.* 263:C1225–C1233.

5. Nielsen, S., B. L. Smith, E. I. Christensen, M. A. Knepper, and P. Agre.

1993. CHIP28 water channels are localized in constitutively water-permeable segments of the nephron. *J. Cell Biol.* 120:371–383.

6. Knepper, M. A. 1994. The aquaporin family of molecular water channels. *Proc. Natl. Acad. Sci. USA.* 91:6255–6258.

7. Smith, B. L., and P. Agre. 1991. Erythrocyte M_r 28,000 transmembrane protein exists as a multisubunit oligomer similar to channel proteins. *J. Biol. Chem.* 266:6407–6415.

8. Maeda, Y., Y. Terada, H. Nonoguchi, and M. A. Knepper. 1992. Hormone and autacoid regulation of cAMP production in rat IMCD subsegments. *Am. J. Physiol.* 263:F319–F327.

9. Wright, P., M. B. Burg, and M. A. Knepper. 1990. Microdissection of kidney tubule segments (chapter 12). *In* Methods in Enzymology. Volume 191. S. Fleischer and B. Fleischer, editors. Academic Press, San Diego. 226–231.

10. Garg, L. C., M. A. Knepper, and M. B. Burg. 1981. Mineralocorticoid effects on Na-K-ATPase in individual nephron segments. *Am. J. Physiol.* 240:F536–F544.

11. Schmidt, D. E., Jr., T. L. Brooks, S. Mhatre, R. P. Junghans, and M. B. Khazaeli. 1993. An advanced solid support for immunoassays and other affinity applications. *Biotechniques.* 14:1020–1025.

12. Knepper, M. A., and F. C. Rector, Jr. 1991. Urinary concentration and dilution (Chapter 12). *In* The Kidney. B. M. Brenner and F. C. Rector, Jr., editors. W. B. Saunders Co., Philadelphia. 445–482.

13. Fushimi, K., S. Uchida, Y. Hara, Y. Hirata, F. Marumo, and S. Sasaki. 1993. Cloning and expression of apical membrane water channel of rat kidney collecting tubule. *Nature (Lond.).* 361:549–552.

14. Nielsen, S., S. R. DiGiovanni, E. I. Christensen, M. A. Knepper, and H. W. Harris, Jr. 1993. Cellular and subcellular immunolocalization of vasopressin-regulated water channel in rat kidney. *Proc. Natl. Acad. Sci. USA.* 90:11663–11667.

15. Nielsen, S., T. L. Pallone, E. I. Christensen, B. L. Smith, P. Agre, and A. B. Maunsbach. 1994. Aquaporin CHIP water channels in rat kidney thin descending limbs and descending vasa recta. *J. Am. Soc. Nephrol.* 5:276 a. (Abstr.)

16. Imai, M., J. Taniguchi, and K. Tabei. 1987. Function of thin loops of Henle. *Kidney Int.* 31:565–579.

17. Preisig, P. A., and C. A. Berry. 1985. Evidence for transcellular osmotic water flow in rat proximal tubules. *Am. J. Physiol.* 249:F124–F131.

18. Green, R., and G. Giebisch. 1989. Reflection coefficients and water permeability in rat proximal tubule. *Am. J. Physiol.* 257:F658–F668.

19. Zeidel, M. L., S. V. Ambudkar, B. L. Smith, and P. Agre. 1992. Reconstitution of functional water channels in liposomes containing purified red cell CHIP28 protein. *Biochemistry.* 31:7436–7440.

20. Van Hoek, A. N., and A. S. Verkman. 1992. Functional reconstitution studies of isolated erythrocyte water channel CHIP28. *J. Biol. Chem.* 267:18267–18269.

21. Maunsbach, A. B., and E. I. Christensen. 1992. Functional ultrastructure of the proximal tubule. *In* Handbook of Physiology. Section 8: Renal Physiology. E. E. Windhager, editor. 41–107.

22. Preston, G. M., B. L. Smith, M. L. Zeidel, J. J. Moulds, and P. Agre. 1994. Mutations in *aquaporin-1* in phenotypically normal humans without functional CHIP water channels. *Science (Wash. DC).* 265:1585–1587.

23. Chou, C.-L., and M. A. Knepper. 1992. In vitro perfusion of chinchilla thin limb segments: segmentation and osmotic water permeability. *Am. J. Physiol.* 263:F417–F426.